# High-pressure sprayed siRNA triggers influence the efficiency but not the profile of transitive silencing

Veli Vural Uslu[1], Athanasios Dalakouras[2,3], Victor A Steffens[1], Gabi Krczal[1], Michael Wassenegger[1,4*]

[1] RLP AgroScience GmbH, 67435 Neustadt an der Weinstraße, Germany

[2] Hellenic Agricultural Organization Demeter, Institute of Industrial and Forage Crops, 41335 Larissa, Greece

[3] Hellenic Agricultural Organization Demeter, Institute of Plant Breeding and Genetic Resources, 57001 Thessaloniki, Greece

[4] Centre for Organismal Studies Heidelberg, University of Heidelberg, 69120 Heidelberg, Germany

*Corresponding author

## ABSTRACT

In plants, small interfering RNAs (siRNAs) are a quintessential class of RNA interference (RNAi)-inducing molecules produced by the endonucleolytic cleavage of double stranded RNAs (dsRNAs). In order to ensure robust RNAi, the siRNAs are amplified through a positive feedback mechanism called transitivity. Transitivity relies on RNA-DIRECTED-RNA POLYMERASE 6 (RDR6)-mediated dsRNA synthesis using siRNA-targeted RNA. This secondary dsRNA is subsequently cleaved into secondary, mainly phased, siRNAs (phasiRNAs) by DICER-LIKE (DCL) endonucleases. As primary siRNAs, secondary siRNAs are also loaded into ARGONAUTE proteins (AGOs) to form an RNA-induced silencing complex (RISC) reinforcing cleavage of the target RNA. Although the molecular players underlying transitivity are well established, the mode of action of transitivity remains elusive. In this study, we investigated the influence of primary target sites on transgene silencing and transitivity using the GFP-expressing *Nicotiana benthamiana* 16C line, high pressure

spraying protocol (HPSP), and synthetic 22-nucleotide (nt) long siRNAs. We found that the siRNA targeting the 3' of the GFP transgene was less efficient in inducing silencing when compared to the siRNAs targeting the 5' and middle region of the GFP. Moreover, sRNA sequencing of locally silenced leaves showed that the amount but not the profile of secondary RNAs are shaped by the occupancy of the primary siRNA triggers on the target RNA. Our findings suggest that RDR6-mediated dsRNA synthesis is not primed by primary siRNAs and that dsRNA synthesis appears to be generally initiated at the 3' end of the target RNA.

## INTRODUCTION

In plants, RNA interference (RNAi) plays a critical role in transcriptional regulation, genome stability and pathogen defense. RNAi is induced upon the presence of double stranded RNAs (dsRNAs) inside the cell. DsRNAs are processed by the endonucleases DICER-LIKE 4 (DCL4), DCL2 and DCL3 into 21-, 22- and 24-nt siRNAs, respectively (Deleris et al. 2006; Fusaro et al. 2006; Blevins et al. 2006). In general, 21-nt siRNAs are loaded onto AGO1 and cleave complementary transcripts, in a process termed post-transcriptional gene silencing (PTGS) (Hamilton and Baulcombe 1999). 22-nt siRNAs are also loaded onto AGO1 and are involved in either the onset of transitivity (see below) (Chen et al. 2010; Cuperus et al. 2010) or translational inhibition (Wu et al. 2020). Finally, 24-nt siRNAs are generally loaded onto AGO4 and the resulting complex is transported into the nucleus, where it reinforces RNA-directed DNA methylation (RdDM) (Chan et al. 2004; Dalakouras and Wassenegger 2013; Wassenegger et al. 1994).

An enzyme of paramount importance in plant RNAi is RNA-DIRECTED RNA POLYMERASE 6 (RDR6). According to a mechanism termed sense-PTGS (S-PTGS), RDR6 is recruited to aberrant RNAs (abRNAs) if the abRNA exceed a certain threshold. The resulting primary dsRNAs are processed into siRNAs, initiating target RNA silencing (Parent et al. 2015; Wassenegger and Krczal, 2006). In addition, it is assumed that RDR6 is recruited

to transcripts that are targeted by (primary) siRNAs for the generation of dsRNA and secondary siRNAs mapping upstream and downstream of the primary siRNA site, a process termed transitivity (Bleys et al. 2006a; Bleys et al. 2006b; Koscianska et al. 2005; Montgomery et al. 2008a; Montgomery et al. 2008b; Vaistij and Jones 2009; Vaistij et al. 2002; Vermeersch et al. 2010; Vermeersch et al. 2013; Moissiard et al. 2007; Mlotshwa et al. 2008; Chen et al. 2010; Cuperus et al. 2010; Manavella et al. 2012).

A growing body of evidence suggests that the onset of transitivity is influenced by the nature of the target transcript. Indeed, transcripts originating from intron-containing genes are poor substrates for RDR6 compared to those derived from intronless ones (Christie et al. 2011a; Christie and Carroll 2011; Christie et al. 2011b; Dadami et al. 2014; Dadami et al. 2013; Liu and Chen 2016; Vermeersch et al. 2010). In addition, transcript expression levels, as well as regulatory elements at the promoter, and/or terminator sequence have been implicated in the efficiency of transitivity (de Felippes and Waterhouse 2020). As noted before, RDR6 transcribes abRNAs which are devoid of 5´ cap and/or 3´ polyadenylation tail (Gazzani et al. 2004; Luo and Chen 2007; Parent et al. 2015). AbRNAs may be produced by both intronless and intron-containing genes e.g. upon read-through transcription or misplicing. In the first case, the abRNAs are processed by RDR6, while in the second case, spliceosome association seems to preferentially recruit the exonucleolytic RNA quality control for their degradation (Christie et al. 2011a; Elvira-Matelot et al. 2016; Tsuzuki et al. 2017; Dalakouras et al. 2019).

Along with the intrinsic features of the target transcript, the sRNA trigger itself appears to affect the initiation and efficiency of transitive silencing. It has been suggested that sRNAs with a size of 22-nt (Chen et al. 2010) or sRNAs containing an asymmetric bulge in their duplex (Manavella et al. 2012) are changing AGO1 conformation thereby recruiting RDR6 to their target, most likely with the aid of a mediator such as SDE3 (Garcia et al. 2012). In line with this, DCL2, responsible for the generation of 22-nt siRNAs, is required for transitivity

initiation (Mlotshwa et al. 2008). Yet, whether 22-nt sRNAs mediate target cleavage, besides RDR6 recruitment, is not clear. Previous reports suggested that RNA cleavage is required for transitivity (Carbonell et al. 2012; Yoshikawa et al. 2005). However, other studies challenge this assumption, arguing that cleavage is dispensable for the onset of transitivity (Arribas-Hernandez et al. 2016; de Felippes et al. 2017).

RDR6 is postulated to initiate transcription predominantly from the very 3′ of the target transcript (Schiebel et al. 1993) and not from an internal site, e.g. the siRNA cleavage site (Moissiard et al. 2007). Furthermore, it has been shown that the 3' cleavage fragment of the abRNA predominantly contributes to the RDR6-mediated transitivity. In contrast, the 5' cleavage fragment, lacking a polyA tail, is subjected to exosome degradation after cleavage, preventing its transcription by RDR6 (Branscheid et al., 2015; Yu et al., 2015). Transitivity spreads both upstream and downstream of the primary siRNA site (Chen et al. 2010; Manavella et al. 2012; McHale et al. 2013; Montgomery et al. 2008b). Yet, transitive spreading is not indefinite, since RDR6 seems to reach its transcriptional limits after approximately 700 nt (Axtell et al. 2006; Moissiard et al. 2007).

Despite considerable progress, the exact mode of action of sRNAs on transitivity remains largely unaddressed (de Felippes and Waterhouse 2020). This is because transitivity studies in plants have been based so far on (1) transgenes expressing hairpin RNAs (hpRNAs) or inverted repeats (IRs), which are processed into a plethora of siRNAs, undermining any attempt to allocate specific roles to discrete siRNAs (Bleys et al. 2006a; Bleys et al. 2006b; Koscianska et al. 2005; Vaistij et al. 2002; Vermeersch et al. 2010; Vermeersch et al. 2013), (2) endogenous micro RNAs (miRNAs), which induce transitivity at very specific endogenous loci and thus exhibit a mode of action hardly reflecting a more generalized process (Axtell et al. 2006; Montgomery et al. 2008a; Montgomery et al. 2008b), and (3) artificial miRNAs (amiRNAs), whose artificial long RNA precursor molecules are generally misprocessed into more than a single amiRNA (Chen et al. 2010; Cuperus et al. 2010;

Manavella et al. 2012; McHale et al. 2013). In order to tackle incongruence and investigate the onset and establishment of transitivity triggered by discrete/unique sRNAs, in this study *in vitro* synthesized 22-nt siRNAs targeting the 5', middle and 3' of a GREEN FLUORESCENT PROTEIN (GFP) transcript were exogenously delivered by High Pressure Spraying Protocol (HPSP) in the GFP-expressing *Nicotiana benthamiana* 16C plant line (Dalakouras et al. 2016; Uslu et al. 2020). The data presented in this study provide novel insights of the mechanistic details of transitivity in plants.

## RESULTS

### SiRNAs targeting 5'-GFP and mid-GFP regions display stronger silencing than 3'-GFP.

We monitored silencing efficiency using the GFP transgene in the *Nicotiana benthamiana* 16C line (Nb-16C) (Voinnet and Baulcombe 1997). We designed three 22-nt long siRNAs (siRNA#164, siRNA#386, and siRNA#739) targeting the 5', middle, and 3' regions of the GFP, respectively (Figure 1a). Each siRNA consists of a double stranded RNA with a 20-nt overlapping sequence, a 5'-phosphate and 2-nt overhangs at the 3' sides which were not methylated. The overlapping sequences possess an uracil-adenine pairing at the end to ensure an effective AGO loading (Czech et al. 2009) (Figure 1a). We applied siRNAs on Nb-16C leaves via HPSP and local silencing phenotypes were evaluated 6 days post spraying (6 dps). 14 out of 14 of the siRNA#164- and siRNA#386-sprayed Nb-16C plants (16C-siR164 and 16C-siR386) showed strong and consistent local silencing. In contrast, 12 out of 14 of the siRNA739-treated plants (16C-siR739) had relatively mild silencing phenotypes, and 2 out of the 14 16C-siR739 displayed no GFP silencing, at all (Fig 1b). Systemic silencing phenotypes were evaluated at 35 dps. 12 out of 14 16C-siR164, 11 out of 14 16C-siR386, and only 1 out of 14 of the 16C-siR739 plants showed systemic silencing (Figure 1c). Hence, 22-nt siRNAs targeting the 5'-GFP and mid-GFP regions resulted in significantly more efficient transgene silencing than the 22-nt siRNAs targeting the 3' GFP region ($p<10^{-4}$).

**SiRNA occupancy influences the amount of generated secondary siRNAs but not their transitivity hotspots**

In order to find out the molecular fingerprints of the three siRNA triggers, we performed sRNA sequencing (sRNA-seq) using leaf samples showing local silencing 6 dps. SRNA-seq revealed the presence of 21-, 22-, and 24-nt secondary sRNAs mapping to the GFP sequence outside of the regions targeted by sprayed siRNAs demonstrating that all three siRNAs led to transitive silencing as early as 6 dps (Figure 2a). The combined normalized profiles of 21-, 22-, and 24-nt long sRNAs in a sliding window of 10 nt revealed multiple secondary siRNA hotspots shared among the different siRNA treatments (see Materials and Methods, sRNA-seq normalization) (Figure 2a). The qualitative profile of sRNA reads obtained by percentage density distribution (pdd, see Materials and Methods, sRNA-seq quantification) also showed several perfectly matching hotspots (Figure 2b). The most prominent secondary siRNA hotspot (Transitivity Hot Spot, THS) appeared as two adjacent peaks between positions +541 and +577 of the GFP cDNA, fully overlapping for all three siRNA treatments (Figure 2a, 2b). Despite the matching hotspots, siRNA#164 treatment produced significantly higher amounts of transitive siRNAs, when compared to siRNA#386 and siRNA#739 ($p<10^{-5}$). In addition, siRNA#386 also resulted in significantly higher amounts of secondary siRNAs than siRNA#739 ($p<10^{-5}$) (Figure 2c). The average distance between two transitivity peaks is measured 23.8bp, with a median value of 21.5bp (Figure 2d).

**Primary siRNA target sites do not influence secondary siRNA distribution**

In order to find out whether primary siRNA binding sites or THS shape the secondary sRNA distribution, we divided the GFP cDNA into 6 regions: 5' region of the siRNA#164 (1-164), the regions between siRNA#164 and siRNA#386 (165-386), siRNA#386 and THS region (387-540), THS and siRNA#739 region (578-739), 3' region of siRNA#739 (740-772), and

the THS region (541-577) itself. The regional percentage distribution of the sRNA-reads (rpd-sRNA, see Materials and Methods, sRNA-seq quantification) show that in the region 1-164, which is 612 bp upstream from the 3'end of the GFP cDNA, contains less than 1% of the reads for all siRNA treatments and there is no statistical difference when different treatments are compared (Figure 3a). A significantly higher portion of secondary siRNAs in 16C-siR164 map to the region 164-386 when compared to these of 16C-siR386 and 16C-siR739. In the 387-540 region, siRNA#164 treatment lead to significantly higher percentage of reads when compared to siRNA#739 but not to siRNA#386. Interestingly, the percentage distribution of the reads in THS does not differ among the siRNA treatments. On the other hand, 16C-siR164 has significantly lower ratio of reads in the 578-739 region, than 16C-siR386 and 16C-siR739 ($p<10^{-4}$) (Figure 3a). Since these regions are different in length, we calculated the average read density per base pair (ARDBP) for each treatment (see Materials and Methods, sRNA quantification) (Figure 3b). None of the siRNA treatments lead to a specific enrichment on the 5' side of the primary target site when compared to the 3' side (Figure 3b). For all three siRNAs treatments, the transitive siRNA distribution per base pair is the highest in THS and ARDBP decreases both on 5' and 3' sides of the THS as the distance of the region to THS increases (Figure 3b). It needs to be noted here, that the sense strand sRNAs reflect both secondary siRNAs and GFP degradation products, whereas the antisense sRNAs must be solely considered as RDR6 transcription products (Uslu et al. 2020). Therefore, strand-specific ARDBP (ssARDBP) is used to distinguish the contribution of sense and anti-sense strands. SsARDBP shows that in regions 164-386, 387-540 and 578-739 of 16C-siR164 and 16C-siR386, mainly antisense secondary siRNAs contribute to minor but statistically significant differences in secondary siRNA enrichment when compared to 16C-siR739 (Figure 3c). Hence, despite having mild differences in secondary siRNA enrichment between the 5' and 3' side of the THS upon different treatments, the overall distribution of secondary siRNAs remained identical in all treatments (Figure 3b, Supplementary Fig 1).

**Secondary siRNA populations are not affected by the primary siRNA target site**

The raw read counts of 21-, 22- and 24-nt reads mapping to the GFP were compared to 21-nt reads mapping to the GFP. 22-nt reads were approximately one third and 24-nt reads were approximately one seventh of the 21-nt reads in all siRNA treatments regardless of the strand polarity (Figure 4a). However, the ratio of 21-nt transitive siRNA reads (normalized to all 21-nt long reads) were equal to the 22-nt secondary siRNAs reads (normalized to all 22-nt reads). Nevertheless, 24-nt reads mapping to the GFP were far less represented in all 24-nt reads, when compared to 21-nt and 22-nt (Figure 4b). In siR164 samples, 21- and 22-nt reads contribute equally to THS (normalized to all 21- and 22-nt reads). However, the ratio of 22- to 21-nt reads in THS in siR164 samples decreases in siR386 samples and decreases even further in siR739 samples (Figure 5). There are multiple peaks like THS, which are more prominent on the sense strand in all treatments (black arrow, Figure 5). Besides, there are a few peaks on the sense strand, specific to 22-nt reads, which are completely absent in the anti-sense strand (purple arrow, Figure 5). We have not detected any particular sequence feature, which may underlie differential representation of the reads on the sense and the anti-sense strands.

**DISCUSSION**

Transitive silencing has been well studied before, but its induction was never analyzed by using unique/discrete siRNAs. We have previously shown that upon HPSP, 22-nt siRNAs were the most potent inducers of local and systemic silencing when compared to 21-nt and 24-nt siRNAs (Dalakouras et al. 2016). In this study, we used 22-nt siRNAs targeting different regions of the GFP transgene in the Nb-16C line to analyze the onset of transitivity by sRNA-seq. Overall, our data showed that 22-nt siRNAs targeting the 5', middle and 3' of the GFP, all induced local silencing and transitivity. Analysis of the locally silenced tissues revealed that the transitivity pattern did not differ among the three different siRNA triggers.

However, the efficiency of transitivity (in terms of the quantity of secondary siRNAs produced) was positively correlated with the gradual proximity of the siRNA trigger towards the 5' of the target (see below). It has been demonstrated before that the generation of secondary dsRNAs/siRNAs not only amplifies/reinforces local silencing, but also mediates the surpassing of a certain threshold required for the onset of systemic silencing (Kalantidis et al. 2006). Indeed, we observed that the gradual siRNA proximity to the 5' led to not only more efficient transitivity but also to more efficient establishment of systemic silencing. These data suggest that transitivity and systemic silencing are tightly connected, although the RNA molecule serving as the actual mobile signal still needs to be identified.

Having a closer look at the generation of the secondary siRNA profiles in the locally silenced tissue provides some interesting insights regarding the mechanistic details of transitivity. (1) All sprayed siRNAs triggered transitivity towards both their 5' and 3', demonstrating that siRNA-mediated transitivity is bi-directional and not uni-directional (Vaistij et al. 2002). (2) Despite their different occupancy on the target, the three applied siRNAs produced very similar transitivity patterns, suggesting that they were not used as primers for RDR6 (otherwise transitivity would have spread only towards the 5' upstream region of each siRNA trigger), corroborating previous reports (Moissiard et al. 2007). (3) In all three siRNA applications, RDR6 transcription started from the very 3' region of the transcript and proceeded towards the 5' for approximately 700 nt (since no secondary siRNAs were detected in the 1-168 region), again in line with previous reports (Moissiard et al. 2007). (4) The homogeneity of the transitivity pattern in all three cases suggests that the starting point from which RDR6 initiated transcription referred to the very 3' region of non-cleaved target transcripts, and not to the 3' end fragments that are generated by RISC-mediated cleavage. Moreover, prematurely terminated transcripts of the GFP that could be considered as abRNA are unlikely serving as templates for RDR6. Accordingly, the role of 22-nt siRNAs would be to predominantly recruit RDR6 to the 3' end of the target rather than mediate target

RNA cleavage (Figure 6). Indeed, 22-nt siRNAs and/or siRNAs exhibiting an asymmetric bulge at their duplex were supposed to change AGO1 conformation (Manavella et al. 2012). This new conformation could not only impair AGO1's RNase activity but could also recruit RDR6 to the 3' of the target transcript, conceivably with the aid of mediators such as SDE3 (Garcia et al. 2012). (5) The accumulating secondary siRNAs were predominantly of 21-nt in size, followed by 22-nt siRNAs and only negligible numbers of 24-nt siRNAs. These findings were in line with previous reports showing that, while all DCLs predominantly co-localize in the nucleus, DCL4 is also present in the cytoplasmic SGS3/RDR6 bodies, thus having privileged access to the RDR6-produced dsRNA (Kumakura et al. 2009; Pontes et al. 2013). (6) Investigating the polarity of secondary siRNA reads, we recorded that they were mainly of sense rather than antisense polarity (compared to the sense target). The reasons for this observation are not very clear, but we speculate that antisense strands, loaded onto AGO1 and exhibiting cleavage activity on the sense target are degraded post-cleavage, while sense strands, having no obvious target in the cell, have a longer half-life (Shi et al., 2020). (7) The fact that the gradual proximity to the 5' end of the target is positively correlated with the efficiency (but not pattern) of secondary siRNA production, seems to reflect a mechanism wherein siRNA/RISC occupancy close to the 3' end sterically hinders RDR6 recruitment to the very 3' end of the target. (8) The fact that no U-only or A-only sRNA reads were detected (which could have been derived from DCL processing of an A/U-only dsRNA) suggests that RDR6 does not process polyA-containing mRNAs. It has been demonstrated that polyA inhibits RDR6 (Baeg et al. 2017). Moreover, it was shown that RDR6 prefers non-polyadenylated transcripts (Luo and Chen 2007). Indeed, RDR6 transcription of polyA would generate U-only siRNAs that could indiscriminately target any polyA-containing mRNA for cleavage, with devastating effects for the plant cell (Dalakouras et al. 2019). Thus, we suggest that in our case, the sprayed 22-nt siRNAs targeted both GFP mRNAs and GFP abRNAs, but seemingly did not efficiently cleave them. To the GFP mRNA, the 22-nt siRNA failed to

recruit RDR6, due to the presence of the polyA, but inhibited its translation (Wu et al. 2020). To the GFP abRNA, RDR6 could be recruited to initiate S-PTGS. However, the Nb-16C line does not show spontaneous silencing indicating that the concentration of abRNA is too low for the initiation of S-PTGS. The presence of 22-nt siRNAs appears to kinetically facilitated RDR6 recruitment to abRNA, culminating in the generation of secondary 21-nt siRNAs that targeted both GFP mRNA and GFP abRNA for degradation and reinforcement of silencing state (Figure 6).

## MATERIALS and METHODS:

### High Pressure Spraying Protocol (HPSP)

14 of 25 days old *Nicotiana benthamiana* 16C (Nb-16C) plants were used for spraying. Given siRNAs are synthesized by Metabion (www.metabion.com) and dissolved in water. For each plant 200µl of aqueous siRNA solution at 1µM concentration is sprayed from a 0.5-1 cm distance at the shoot apical meristem and at the abaxial surface of the leaves with an airbrush pistol (CONRAD AFC-250A, 0.25mm nozzle). 5-6 bar pressure is provided by the METABO Elektra Beckum Classic 250 compressor for spraying (www.metabo.com). For each siRNA a separate unused airbrush is used to prevent cross-contamination. Furthermore, at the time of spraying only one set of plants (14 plants) were present in the room and they were covered with a transparent plastic hood subsequent to spraying to prevent siRNA cross-contamination through aerosols.

### Ultraviolet (UV) Monitoring

GFP expressing Nb-16C plants were visualized 6 days post spraying (dps) under UV light (Blak-Ray B-100 AP Lamp, www.uvp.com). Images were taken using a Canon EOS700D

(18-55mm), aperture priority mode (A=10). First systemic silencing appeared 14 dps and GFP monitoring was weekly performed up to 35dps.

**RNA Extraction and Small RNA Sequencing**

6 dps, 1 leaf per plant from three plants were pooled as one biological replicate of a sRNA-seq sample. The silenced parts of the leaves were cut out. Three samples per siRNA spraying were collected. The other sprayed leaves were left on the plant to monitor the development of systemic silencing. SRNAs were extracted by mirVana miRNA extraction kit according to manufacturer's instructions (www.thermofisher.com). 250 ng of RNA per biological replicate were provided to GenXPro GmbH for sRNA-seq. GenXPro used TrueQuant SmallRNA Seq Kit for library preparation (https://genxpro.net/). Illumina NextSeq500 instrument was used for sequencing the libraries with 75 cycles of sequencing. As expected from previous reports, sRNA-seq quality control show that 24- and 21-nt reads are the most abundant reads (Blevins et al. 2015, Uslu et al. 2020).

**Bioinformatic Analysis**

SRNA-seq reads are mapped to the GFP sequence of the Nb-16C (Philips et al., 2017). The bam files are visualized on TABLET® (Milne et al. 2013) and the following data processing and line charts/bar graphs have been plotted using Microsoft Excel.

**Elimination of aerosol based cross-contamination upon spraying**

When siRNAs are sprayed not all of them enter the plant cells and most likely, the majority of them stick to the surface of the leaves. In addition, a reasonable amount of siRNAs will, as aerosolic particles, contaminate other non-sprayed plants. Despite all efforts to block cross-contamination via aerosols upon spraying, in all plants we could still detect siRNAs, which were not sprayed to this particular plant but some others. In order to assess the contribution of

this aerosol based cross contamination, we sprayed 3 Nb-16C plants with an siRNA mapping to the promoter sequence of the GFP (siRNA-35S). Upon sequencing of these control plants, we could detect previously sprayed siRNAs, namely siRNA#164, siRNA#386, siRNA#739. However, we never monitored any contamination-based GFP silencing. Moreover, sRNA-seq data of siRNA-35S-sprayed Nb-16C samples did not reveal secondary siRNAs or any other anti-sense sRNA mapping to the GFP sequences. This suggests that the contaminating siRNAs did not contribute to transitivity (data not shown). In order to focus on the secondary siRNAs only, we eliminated all reads mapping to siRNA164, siRNA386, and siRNA739. It should be noted that the sprayed siRNAs represented the far most (91% to 98%) of all reads mapping to the GFP. This underpins the assumption that most of the sprayed siRNAs stick to the leaf surface.

**SRNA-seq Normalization**

Since there are currently no established protocols for normalizing the reads, we used miRNA159 abundance, average and geometric average reads of 3 independent miRNAs, sprayed siRNA abundance, total number of reads, total number of 21-nt reads, total GFP sense reads, NOS terminator reads as a reference to normalize the sRNA reads mapping to the GFP (data not shown). However, the variance among biological replicates were too high to obtain any meaningful comparison between different treatments. Finally, we normalized sRNAs mapping to the GFP sequence with the total number of sRNAs of given size. Namely, 21-nt long reads mapping to the GFP were normalized to the number of all 21-nt reads. We obtained the lowest variance among biological replicates using this size-based normalization. Normalized average read counts refer to this number multiplied with $10^6$ (Figure 2a, 2c, 4b, 5).

**SRNA-seq quantification**

Percent density distribution (pdd) is calculated by dividing the sum of 21-, 22-, and 24-nt reads mapping to the given position to the total number of 21-, 22-, and 24-nt reads mapping to the GFP (Figure 2b). Pdd gives an accurate comparison of the distribution of secondary siRNAs among different treatments, allowing us to compare the treatments qualitatively, regardless of the total abundance of transitive siRNAs. Regional percent distribution of 21-, 22-, 24-nt reads (rpd-sRNA) is obtained by dividing the number of 21-, 22-, and 24-nt reads mapping to the region of interest given in the X-axis to the total number of 21-, 22- and 24-nt reads mapping to the GFP. However, we obtain higher values of rpd-sRNA for larger regions. In order to avoid the size-bias, we calculated average read density per base pair (ARDBP). For ARDBP, we normalized strand specific rpd-sRNA for each region given in the X-axis by the size of the region. ARDBP allows comparison of transitivity distribution of different treatments in a quantitative manner (Figure 3b). The abundance of 21-, 22-, and 24-nt long sRNAs are compared by simply dividing the raw read counts of the sRNAs mapping to GFP to the raw read counts of the 21-nt long sRNAs mapping to GFP (Figure 4a). Next, we evaluated the abundance of 21-, 22-, and 24-nt sRNAs mapping to the GFP normalized with the total number of corresponding size sRNA along the GFP (Figure 4b)

**Statistical Tests**

The statistical comparison of systemic silencing efficiency among different treatments were performed by Fisher's Exact Test with a significance threshold of $p<0.0001$ (Figure 1c). The statistical analysis pdsRNA, ARDBP, and pdd are performed by pairwise comparisons using student's t-test. The significance thresholds are: $p<0.05$(*), $p<0.01$(**), and $p<0.001$(***).

**Author Contributions**

VVU, GK, AD and MW conceived the experiments and wrote the manuscript. VVU and conducted all the experiments and analyzed the data. VAS contributed to the bioinformatic analysis of the sRNA-seq. All authors contributed to the article and approved the submitted version.

**Funding**

Funding of this project was provided by the German Research Foundation (DFG), Grant: Wa1019/14-1 and by the Federal Ministry of Education and Research (BMBF), Grant: 03180531.

**Conflict of Interest**

The authors declare that the research was conducted in the absence of any commercial or financial relationships that could be construed as a potential conflict of interest.

**Figure Legends**

**Figure 1| Silencing phenotypes obtained by siRNAs**. (a) 35S promoter (p35S), Green Fluorescent Protein 5 coding region (GFP5) and NOPALINE SYNTHASE terminator (tNOS) is shown. The exact location of where siRNA#164, siRNA#386, and siRNA739 map on the GFP are provided as #164-188, #386-410, #739-763, respectively. The RNA duplex sequences of the siRNAs with 3' 2 nt overhangs are provided and U-A base pairing at the 5' ends are shown in red letters. (b) The upper panel shows the whole plants sprayed with the corresponding siRNAs, imaged under the UV light. Fully GFP expressing plants have green stems, orange leaves. The silenced areas appear in red. The lower panel shows the silenced leaves under UV, lights. The red silenced areas were excised and used for sRNA-seq. (c) The table shows the distribution of the local silencing at 6 dps and systemic silencing at 35 dps for the given sRNA treatments. The statistical comparison of siRNA#739 and the other two siRNAs are performed by Fisher's Exact Test (***, $p<10^{-4}$)

**Figure2| Quantity and quantitative distribution of transitive siRNAs along GFP.** (a) The graph shows normalized read counts of 21-, 22- and 24-nt combined along GFP. Each of 21-, 22-, and 24-nt reads mapping to the GFP is normalized to total 21-, 22-, and 24-nt reads in the sample and multiplied with $10^6$ for each position along the GFP. These normalized values of 21-, 22- and 24-nt siRNAs are summed up for each biological replicate and the average value of the biological replicates are shown in a sliding window of 10 nt. In the X-axis, the translational start site, the stop codon and the position, where the siRNAs map are provided together with Transitivity Hot Spot (THS). (b) Percent density distribution (pdd) is calculated

for each position (see Materials and Methods). The average pdd values of biological replicates are plotted in a sliding window of 10 nt and the percentage values for each position is given in Y-axis. The relevant positions along the GFP are given in X-axis. (c) The normalized counts of combined 21-, 22-, and 24-nt long reads mapping to GFP are plotted for each siRNA treatment. The values of each biological replicate are shown as data points in the bar chart. Student's t-test is used for pairwise comparison (***, $p<10^{-3}$). (d) The distance between the peaks, shared among all three siRNA treatments are calculated and provided in a bar chart. Horizontal axis shows the distance in the unit of base pairs. In all the charts and graphs, siRNA#164 is shown in blue, siRNA#386 in orange, and siRNA#739 is grey.

**Figure 3| Regional and strand-specific distribution of transitive siRNAs.** (a) Regional percent distribution of 21-, 22- and 24-nt reads (rpd-sRNA, see Materials and Methods) between the positions given in the X-Axis in addition to THS, which is taken as a separate area. For each treatment, the average rpd-sRNA of three biological replicates are plotted. The error bars indicate standard deviation and student's t-test is used for pairwise statistical comparison between different siRNA treatments. (b) In order to avoid size-bias in rpd-sRNA, average percent read density per base pair (ARDPB, see Materials and Methods) is plotted to compare the rpd-sRNA between different regions for each siRNA treatment. The ARDPB decreases as the region is further away from THS for all siRNA treatments. The position of the siRNAs used for the experiment is shown in the X-axis with respect to the six regions of interest. (c) Strand specific ARDPB is plotted for the regions given in the X-axis. Y axis shows the ARDPB in terms of percent probability for sense (bars with solid colours above the X-axis, and bars with diagonal patterns below the X-axis). Student t-test is used for pairwise comparisons between siRNA treatments in the given region. In all the charts siRNA#164 is shown in blue, siRNA#386 in orange, and siRNA#739 in grey.

**Figure 4| Comparison of 21-, 22- and 24-nt transitive siRNAs.** (a) Average of total 21-, 22-, and 24-nt reads mapping to GFP normalized to 21-nt reads mapping to GFP of three biological replicate upon siRNA treatments. Regardless of the siRNA treatment, 22-nt reads are one third of the 21-nt reads and 24-nt reads are one seventh of the 21-nt reads on both sense (solid colours above X-axis) and anti-sense strand (diagonal pattern below X-axis). (b) The ratio of 21-, 22- and 24-nt reads mapping to GFP regardless of the strand, normalized to the total number of sRNAs of 21-, 22- and 24-nt siRNA reads, respectively, for each position on GFP. The value is multiplied with $10^6$ and the graph is plotted in a sliding window of 10 nt. siRNA#164 treatment is shown in blue, siRNA#386 in orange, and siRNA739 in grey. From the darkest to the lightest tone of each colour, 21-, 22-, and 24-nt long reads are plotted, respectively.

**Figure 5| Strand Specific Distribution of 21- and 22-nt transitive siRNAs.** The ratio of 21-, 22- and 24-nt siRNA reads mapping to GFP, normalized to the total number of sRNAs of 21-, 22- and 24-nt siRNA reads, respectively, for each position on GFP. The value is multiplied with $10^6$ and the graph is plotted in a sliding window of 10 nt in a strand specific manner. Sense strand is plotted with a solid line above the X-axis with and anti-sense strand is plotted with a dotted line below the X-axis. Black arrows show the THS peak, which is more prominent on the sense strand, whereas purple arrow depicts a 22-nt siRNA read peak in the sense strand, which is lacking in the anti-sense strand.

**Figure 6| A model for the role of siRNAs in transitivity.** A plant gene may generate either legitimate mRNAs or aberrant RNAs (abRNAs) that lack a 5' cap structure and/or a 3' polyadenylation tail. In the absence of siRNAs, mRNAs are translated into protein, whereas abRNAs, posing a potential deleterious effect on the plant cell, are channeled (primarily) to

RDR6-mediated decay (sense PTGS) and (secondarily) to competing exonucleolytic RNA decay pathways. In the presence of 21-nt siRNAs, both mRNAs and abRNAs are targeted and cleaved by 21-nt siRNAs (PTGS). The cleavage products are not processed, at least significantly, by RDR6, but are rapidly degraded by exonucleolytic pathways (as typically happens in the case of 21-nt miRNA cleavage products). In the presence of 22-nt siRNAs, AGO1 conformation is seemingly affected by 22-nt siRNA loading (or by small RNAs containing an asymmetric bulge) and this impairs AGO/RISC capacity for cleavage. Instead, AGO1-loaded 22-nt siRNAs inhibit translation of mRNAs and recruit RDR6 to the 3' end of abRNAs, possibly with a mediator such as SDE3, and for a distance of approximately 700 nt, generating 21-nt secondary siRNAs (transitivity). These secondary 21-nt siRNAs cleave homologous mRNAs and abRNAs (local PTGS) and can be transported through the plasmodesmata to neighboring cells. Importantly, during the process of transitivity, an RNA signal of yet unidentified nature is generated and transported through the phloem to establish systemic PTGS to distant parts of the plant. In this model RDR6 processes only abRNA and not mRNAs. Indeed, polyadenylation tails were shown to inhibit RDR6 transcription, a meaningful evolutionary strategy to avoid generation of U-only siRNAs which could indiscriminately target any given mRNA for PTGS.

**Supplementary Table1|** sRNA-seq quality control. Total read numbers and 21, 22, and 24nt read numbers given in the table. In addition, the 22nt reads matching exactly to sprayed RNAs are provided.

**Supplementary Figure 1|** The normalized 21,22, and 24nt mapping to the 5' side of the THS is normalized to the 3' side of the THS on both strands for three siRNA treatments. (***, $p<0.01$)

**REFERENCES.**


Arribas-Hernandez L, Marchais A, Poulsen C, Haase B, Hauptmann J, Benes V, Meister G, Brodersen P (2016) The Slicer Activity of ARGONAUTE1 Is Required Specifically for the Phasing, Not Production, of Trans-Acting Short Interfering RNAs in Arabidopsis. The Plant cell 28 (7):1563-1580

Axtell MJ, Jan C, Rajagopalan R, Bartel DP (2006) A two-hit trigger for siRNA biogenesis in plants. Cell 127 (3):565-577

Baeg K, Iwakawa HO, Tomari Y (2017) The poly(A) tail blocks RDR6 from converting self mRNAs into substrates for gene silencing. Nat Plants 3:17036. doi:10.1038/nplants.2017.36

Blevins T, Rajeswaran R, Shivaprasad PV, Beknazariants D, Si-Ammour A, Park HS, Vazquez F, Robertson D, Meins F, Jr., Hohn T, Pooggin MM (2006) Four plant Dicers mediate viral small RNA biogenesis and DNA virus induced silencing. Nucleic acids research 34 (21):6233-6246

Blevins T, Podicheti R, Mishra V, Marasco M, Wang J, Rusch D, Tang H, Pikaard CS (2015) Identification of Pol IV and RDR2-dependent precursors of 24 nt siRNAs guiding de novo DNA methylation in Arabidopsis. Elife. 4:e09591.

Bleys A, Van Houdt H, Depicker A (2006a) Down-regulation of endogenes mediated by a transitive silencing signal. RNA (New York, NY 12 (9):1633-1639

Bleys A, Vermeersch L, Van Houdt H, Depicker A (2006b) The frequency and efficiency of endogene suppression by transitive silencing signals is influenced by the length of sequence homology. Plant physiology 142 (2):788-796

Branscheid A, Marchais A, Schott G, Lange H, Gagliardi D, Andersen SU, Voinnet O, Brodersen P (2015) SKI2 mediates degradation of RISC 5'-cleavage fragments and prevents secondary siRNA production from miRNA targets in Arabidopsis. Nucleic Acids Res. 43(22):10975-88. doi: 10.1093/nar/gkv1014.

Carbonell A, Fahlgren N, Garcia-Ruiz H, Gilbert KB, Montgomery TA, Nguyen T, Cuperus JT, Carrington JC (2012) Functional analysis of three Arabidopsis ARGONAUTES using slicer-defective mutants. The Plant cell 24 (9):3613-3629

Chan SW, Zilberman D, Xie Z, Johansen LK, Carrington JC, Jacobsen SE (2004) RNA silencing genes control de novo DNA methylation. Science 303 (5662):1336. doi:10.1126/science.1095989

Chen HM, Chen LT, Patel K, Li YH, Baulcombe DC, Wu SH (2010) 22-Nucleotide RNAs trigger secondary siRNA biogenesis in plants. Proc Natl Acad Sci U S A 107 (34):15269-15274. doi:10.1073/pnas.1001738107

Christie M, Brosnan CA, Rothnagel JA, Carroll BJ (2011a) RNA decay and RNA silencing in plants: competition or collaboration? Front Plant Sci 2:99

Christie M, Carroll BJ (2011) SERRATE is required for intron suppression of RNA silencing in Arabidopsis. Plant Signal Behav 6 (12):2035-2037

Christie M, Croft LJ, Carroll BJ (2011b) Intron splicing suppresses RNA silencing in Arabidopsis. Plant J 68 (1):159-167. doi:10.1111/j.1365-313X.2011.04676.x

Cuperus JT, Carbonell A, Fahlgren N, Garcia-Ruiz H, Burke RT, Takeda A, Sullivan CM, Gilbert SD, Montgomery TA, Carrington JC (2010) Unique functionality of 22-nt miRNAs in triggering RDR6-dependent siRNA biogenesis from target transcripts in Arabidopsis. Nat Struct Mol Biol 17 (8):997-1003. doi:10.1038/nsmb.1866

Czech B, Zhou R, Erlich Y, Brennecke J, Binari R, Villalta C, Gordon A, Perrimon N, Hannon GJ (2009) Hierarchical rules for Argonaute loading in Drosophila. Mol Cell. 13;36(3):445-56. doi: 10.1016/j.molcel.2009.09.028.

Dadami E, Dalakouras A, Zwiebel M, Krczal G, Wassenegger M (2014) An endogene-resembling transgene is resistant to DNA methylation and systemic silencing. RNA Biol 11 (7):934-941. doi:10.4161/rna.29623

Dadami E, Moser M, Zwiebel M, Krczal G, Wassenegger M, Dalakouras A (2013) An endogene-resembling transgene delays the onset of silencing and limits siRNA accumulation. FEBS letters 18 (587(6)):706-710

Dalakouras A, Lauter A, Bassler A, Krczal G, Wassenegger M (2019) Transient expression of intron-containing transgenes generates non-spliced aberrant pre-mRNAs that are processed into siRNAs. Planta 249 (2):457-468. doi:10.1007/s00425-018-3015-6

Dalakouras A, Wassenegger M (2013) Revisiting RNA-directed DNA methylation. RNA Biol 10 (3):453-455. doi:10.4161/rna.23542

Dalakouras A, Wassenegger M, McMillan JN, Cardoza V, Maegele I, Dadami E, Runne M, Krczal G, Wassenegger M (2016) Induction of Silencing in Plants by High-Pressure Spraying of In vitro-Synthesized Small RNAs. Front Plant Sci 7:1327. doi:10.3389/fpls.2016.01327

de Felippes FF, Marchais A, Sarazin A, Oberlin S, Voinnet O (2017) A single miR390 targeting event is sufficient for triggering TAS3-tasiRNA biogenesis in Arabidopsis. Nucleic acids research

de Felippes FF, Waterhouse PM (2020) The Whys and Wherefores of Transitivity in Plants. Front Plant Sci 11:579376. doi:10.3389/fpls.2020.579376

Deleris A, Gallego-Bartolome J, Bao J, Kasschau KD, Carrington JC, Voinnet O (2006) Hierarchical action and inhibition of plant Dicer-like proteins in antiviral defense. Science (New York, NY 313 (5783):68-71

Elvira-Matelot E, Bardou F, Ariel F, Jauvion V, Bouteiller N, Le Masson I, Cao J, Crespi MD, Vaucheret H (2016) The Nuclear Ribonucleoprotein SmD1 Interplays with Splicing, RNA Quality Control, and Posttranscriptional Gene Silencing in Arabidopsis. The Plant cell 28 (2):426-438

Fusaro AF, Matthew L, Smith NA, Curtin SJ, Dedic-Hagan J, Ellacott GA, Watson JM, Wang MB, Brosnan C, Carroll BJ, Waterhouse PM (2006) RNA interference-inducing hairpin RNAs in plants act through the viral defence pathway. EMBO Rep 7 (11):1168-1175. doi:10.1038/sj.embor.7400837

Garcia D, Garcia S, Pontier D, Marchais A, Renou JP, Lagrange T, Voinnet O (2012) Ago hook and RNA helicase motifs underpin dual roles for SDE3 in antiviral defense and silencing of nonconserved intergenic regions. Mol Cell 48 (1):109-120. doi:10.1016/j.molcel.2012.07.028

Gazzani S, Lawrenson T, Woodward C, Headon D, Sablowski R (2004) A link between mRNA turnover and RNA interference in Arabidopsis. Science 306 (5698):1046-1048. doi:10.1126/science.1101092

Hamilton AJ, Baulcombe DC (1999) A species of small antisense RNA in posttranscriptional gene silencing in plants. Science 286 (5441):950-952

Kalantidis K, Tsagris M, Tabler M (2006) Spontaneous short-range silencing of a GFP transgene in Nicotiana benthamiana is possibly mediated by small quantities of siRNA that do not trigger systemic silencing. Plant J 45 (6):1006-1016. doi:10.1111/j.1365-313X.2006.02664.x

Koscianska E, Kalantidis K, Wypijewski K, Sadowski J, Tabler M (2005) Analysis of RNA silencing in agroinfiltrated leaves of Nicotiana benthamiana and Nicotiana tabacum. Plant Mol Biol 59 (4):647-661. doi:10.1007/s11103-005-0668-x

Kumakura N, Takeda A, Fujioka Y, Motose H, Takano R, Watanabe Y (2009) SGS3 and RDR6 interact and colocalize in cytoplasmic SGS3/RDR6-bodies. FEBS Lett 583 (8):1261-1266. doi:10.1016/j.febslet.2009.03.055

Liu L, Chen X (2016) RNA Quality Control as a Key to Suppressing RNA Silencing of Endogenous Genes in Plants. Molecular plant 9 (6):826-836

Luo Z, Chen Z (2007) Improperly terminated, unpolyadenylated mRNA of sense transgenes is targeted by RDR6-mediated RNA silencing in Arabidopsis. The Plant cell 19 (3):943-958

Manavella PA, Koenig D, Weigel D (2012) Plant secondary siRNA production determined by microRNA-duplex structure. Proc Natl Acad Sci U S A 109 (7):2461-2466. doi:10.1073/pnas.1200169109

McHale M, Eamens AL, Finnegan EJ, Waterhouse PM (2013) A 22-nt artificial microRNA mediates widespread RNA silencing in Arabidopsis. Plant J 76 (3):519-529. doi:10.1111/tpj.12306

Milne I, Stephen G, Bayer M, Cock PJ, Pritchard L, Cardle L, Shaw P,Marshall D (2013) Using Tablet for visual exploration of secondgeneration sequencing data. Brief Bioinform 14:193–202.

Mlotshwa S, Pruss GJ, Peragine A, Endres MW, Li J, Chen X, Poethig RS, Bowman LH, Vance V (2008) DICER-LIKE2 plays a primary role in transitive silencing of transgenes in Arabidopsis. PloS one 3 (3):e1755

Moissiard G, Parizotto EA, Himber C, Voinnet O (2007) Transitivity in Arabidopsis can be primed, requires the redundant action of the antiviral Dicer-like 4 and Dicer-like 2, and is compromised by viral-encoded suppressor proteins. RNA (New York, NY 13 (8):1268-1278

Montgomery TA, Howell MD, Cuperus JT, Li D, Hansen JE, Alexander AL, Chapman EJ, Fahlgren N, Allen E, Carrington JC (2008a) Specificity of ARGONAUTE7-miR390 interaction and dual functionality in TAS3 trans-acting siRNA formation. Cell 133 (1):128-141

Montgomery TA, Yoo SJ, Fahlgren N, Gilbert SD, Howell MD, Sullivan CM, Alexander A, Nguyen G, Allen E, Ahn JH, Carrington JC (2008b) AGO1-miR173 complex initiates phased siRNA formation in plants. Proceedings of the National Academy of Sciences of the United States of America 105 (51):20055-20062

Parent JS, Jauvion V, Bouche N, Beclin C, Hachet M, Zytnicki M, Vaucheret H (2015) Post-transcriptional gene silencing triggered by sense transgenes involves uncapped antisense RNA and differs from silencing intentionally triggered by antisense transgenes. Nucleic Acids Res 43 (17):8464-8475. doi:10.1093/nar/gkv753

Philips JG, Naim F, Lorenc MT, Dudley KJ, Hellens RP, Waterhouse PM (2017) The widely used Nicotiana benthamiana 16c line has an unusual T-DNA integration pattern including a transposon sequence. PLoS One. 23;12(2):e0171311. doi: 10.1371/journal.pone.0171311.

Pontes O, Vitins A, Ream TS, Hong E, Pikaard CS, Costa-Nunes P (2013) Intersection of small RNA pathways in Arabidopsis thaliana sub-nuclear domains. PLoS One 8 (6):e65652. doi:10.1371/journal.pone.0065652

Schiebel W, Haas B, Marinkovic S, Klanner A, Sanger HL (1993) RNA-directed RNA polymerase from tomato leaves. II. Catalytic in vitro properties. The Journal of biological chemistry 268 (16):11858-11867

Shi CY, Kingston, ER, Kleaveland, B, Lin DH, Stubna MW, Bartel, DP (2020) The ZSWIM8 ubiquitin ligase mediates target-directed microRNA degradation. *Science (New York, N.Y.)*, *370*(6523), eabc9359

Tsuzuki M, Motomura K, Kumakura N, Takeda A (2017) Interconnections between mRNA degradation and RDR-dependent siRNA production in mRNA turnover in plants. J Plant Res 130 (2):211-226

Uslu VV, Bassler A, Krczal G, Wassenegger M (2020) High-Pressure-Sprayed Double Stranded RNA Does Not Induce RNA Interference of a Reporter Gene. Front Plant Sci 11:534391. doi:10.3389/fpls.2020.534391

Vaistij FE, Jones L (2009) Compromised virus-induced gene silencing in RDR6-deficient plants. Plant physiology 149 (3):1399-1407

Vaistij FE, Jones L, Baulcombe DC (2002) Spreading of RNA targeting and DNA methylation in RNA silencing requires transcription of the target gene and a putative RNA-dependent RNA polymerase. Plant Cell 14 (4):857-867. doi:10.1105/tpc.010480

Vermeersch L, De Winne N, Depicker A (2010) Introns reduce transitivity proportionally to their length, suggesting that silencing spreads along the pre-mRNA. Plant J 64 (3):392-401

Vermeersch L, De Winne N, Nolf J, Bleys A, Kovarik A, Depicker A (2013) Transitive RNA silencing signals induce cytosine methylation of a transgenic but not an endogenous target. Plant J 74 (5):867-879

Voinnet O, Baulcombe DC (1997) Systemic signalling in gene silencing. Nature 389 (6651):553. doi:10.1038/39215

Wassenegger M, Heimes S, Riedel L, Sanger HL (1994) RNA-directed de novo methylation of genomic sequences in plants. Cell 76 (3):567-576. doi:10.1016/0092-8674(94)90119-8

Wassenegger M, Krczal G (2006) Nomenclature and functions of RNA-directed RNA polymerases. Trends in plant science, 11(3), 142–151. https://doi.org/10.1016/j.tplants.2006.01.003

Wu H, Li B, Iwakawa H, Pan Y, Tang X, Ling-hu Q, Liu Y, Sheng S, Feng L, Zhang H, Zhang X, Tang Z, Xia X, Zhai J, Guo H (2020a) Plant 22-nt siRNAs mediate translational repression and stress adaptation. Nature. doi:10.1038/s41586-020-2231-y

Yoshikawa M, Peragine A, Park MY, Poethig RS (2005) A pathway for the biogenesis of trans-acting siRNAs in Arabidopsis. Genes & development 19 (18):2164-2175

Yu A, Saudemont B, Bouteiller N, Elvira-Matelot E, Lepère G, Parent JS, Morel JB, Cao J, Elmayan T, Vaucheret H (2015) Second-Site Mutagenesis of a Hypomorphic argonaute1 Allele Identifies SUPERKILLER3 as an Endogenous Suppressor of Transgene Posttranscriptional Gene Silencing. Plant Physiol. 169(2):1266-74. doi: 10.1104/pp.15.00585.

## FIGURES and SUPPLEMENTARY INFORMATION

Figure 1|

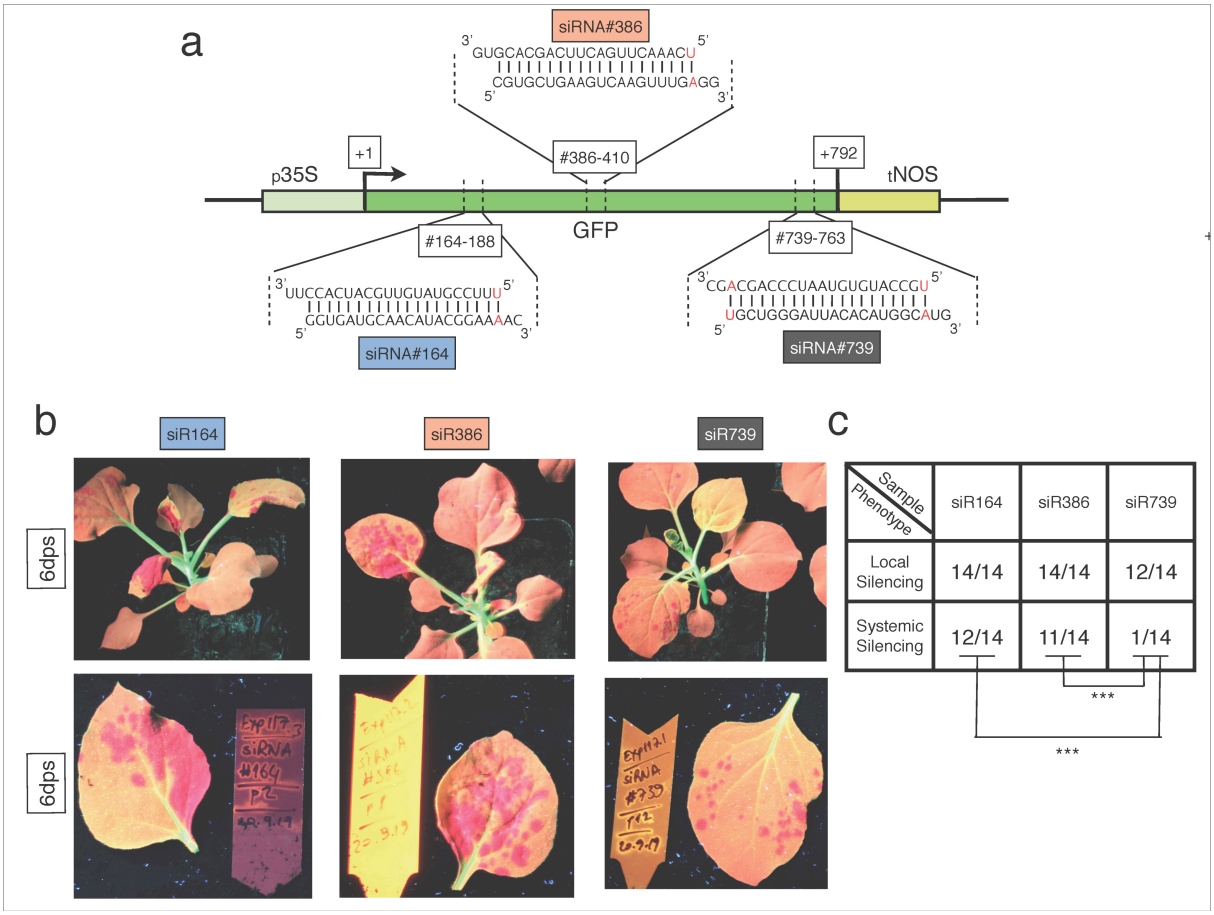

Figure 2|

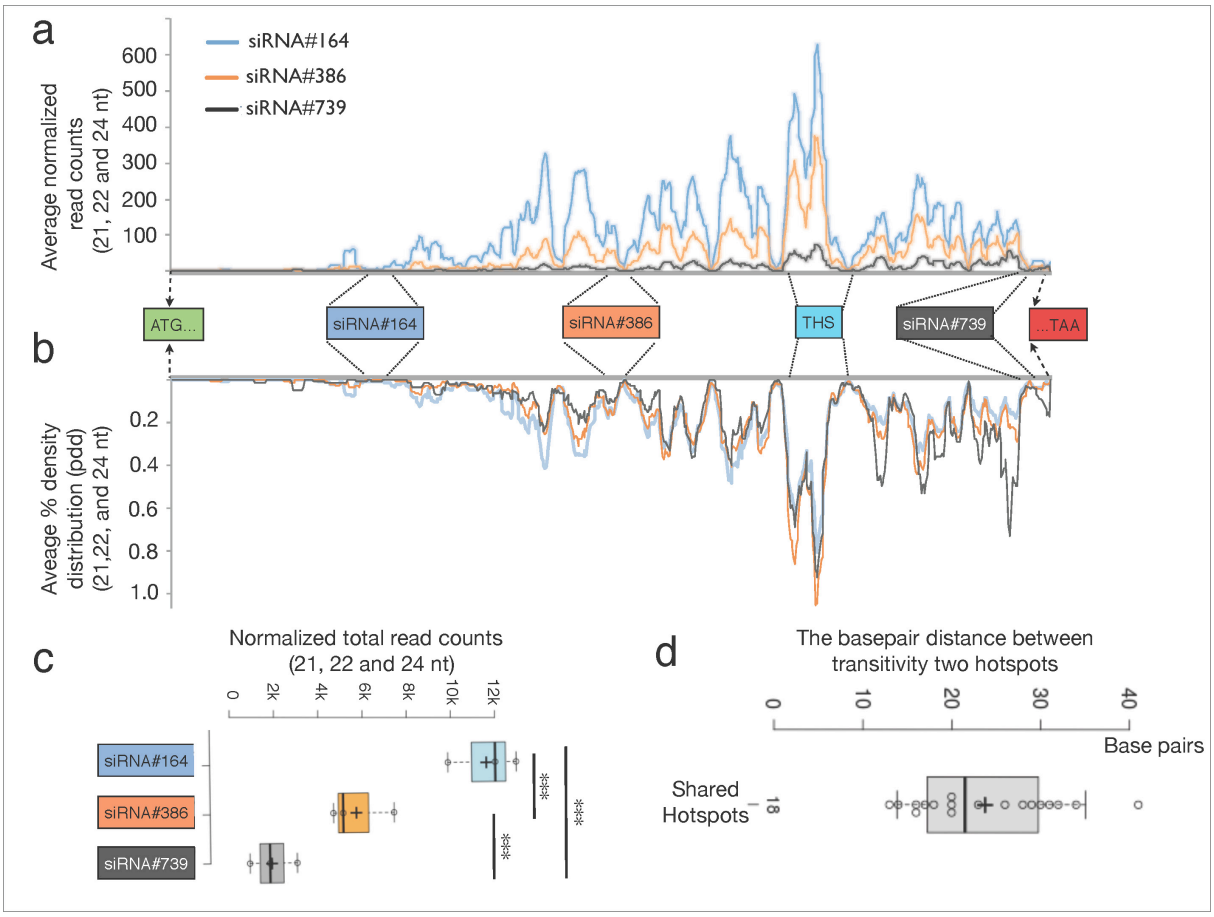
a
siRNA#164
siRNA#386
siRNA#739
Average normalized read counts (21, 22 and 24 nt)
600
500
400
300
200
100
ATG...
siRNA#164
siRNA#386
THS
siRNA#739
...TAA
b
Aveage % density distribution (pdd) (21,22, and 24 nt)
0.2
0.4
0.6
0.8
1.0
c
Normalized total read counts (21, 22 and 24 nt)
0
2k
4k
6k
8k
10k
12k
siRNA#164
siRNA#386
siRNA#739
***
***
***
d
The basepair distance between transitivity two hotspots
0
10
20
30
40
Base pairs
Shared Hotspots
18

Figure 3|

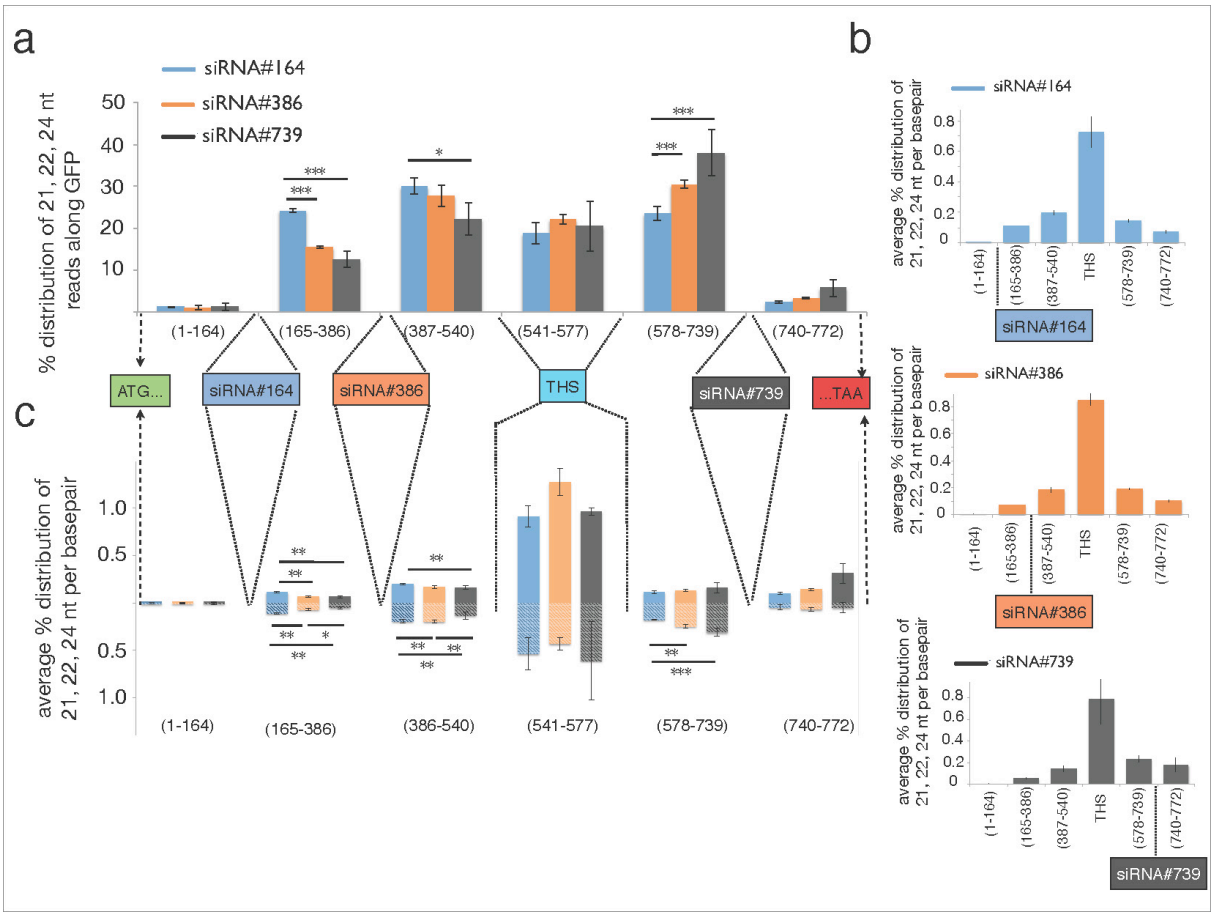
a
siRNA#164
siRNA#386
siRNA#739
% distribution of 21, 22, 24 nt reads along GFP
50
40
30
20
10
(1-164)
(165-386)
(387-540)
(541-577)
(578-739)
(740-772)
ATG...
siRNA#164
siRNA#386
THS
siRNA#739
...TAA
c
average % distribution of 21, 22, 24 nt per basepair
1.0
0.5
0.5
1.0
(1-164)
(165-386)
(386-540)
(541-577)
(578-739)
(740-772)
b
siRNA#164
siRNA#386
siRNA#739
average % distribution of 21, 22, 24 nt per basepair
0.8
0.6
0.4
0.2
0
(1-164)
(165-386)
(387-540)
THS
(578-739)
(740-772)

Figure 4|

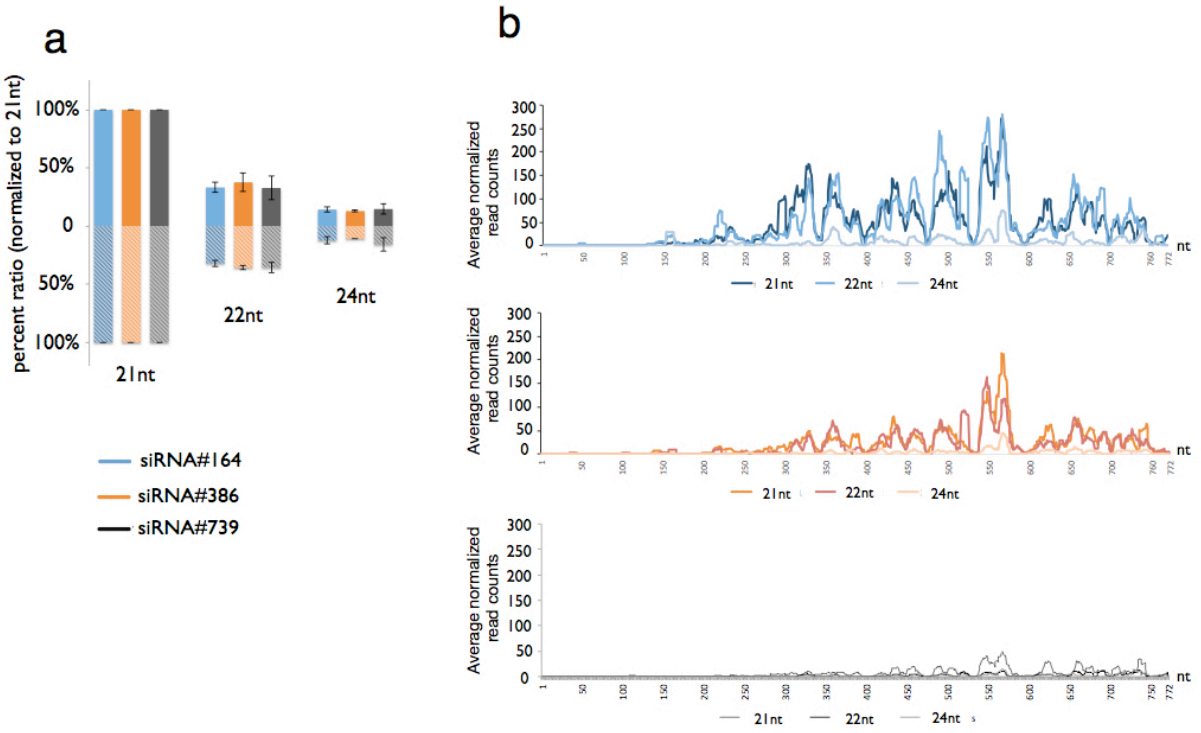


Figure 5|

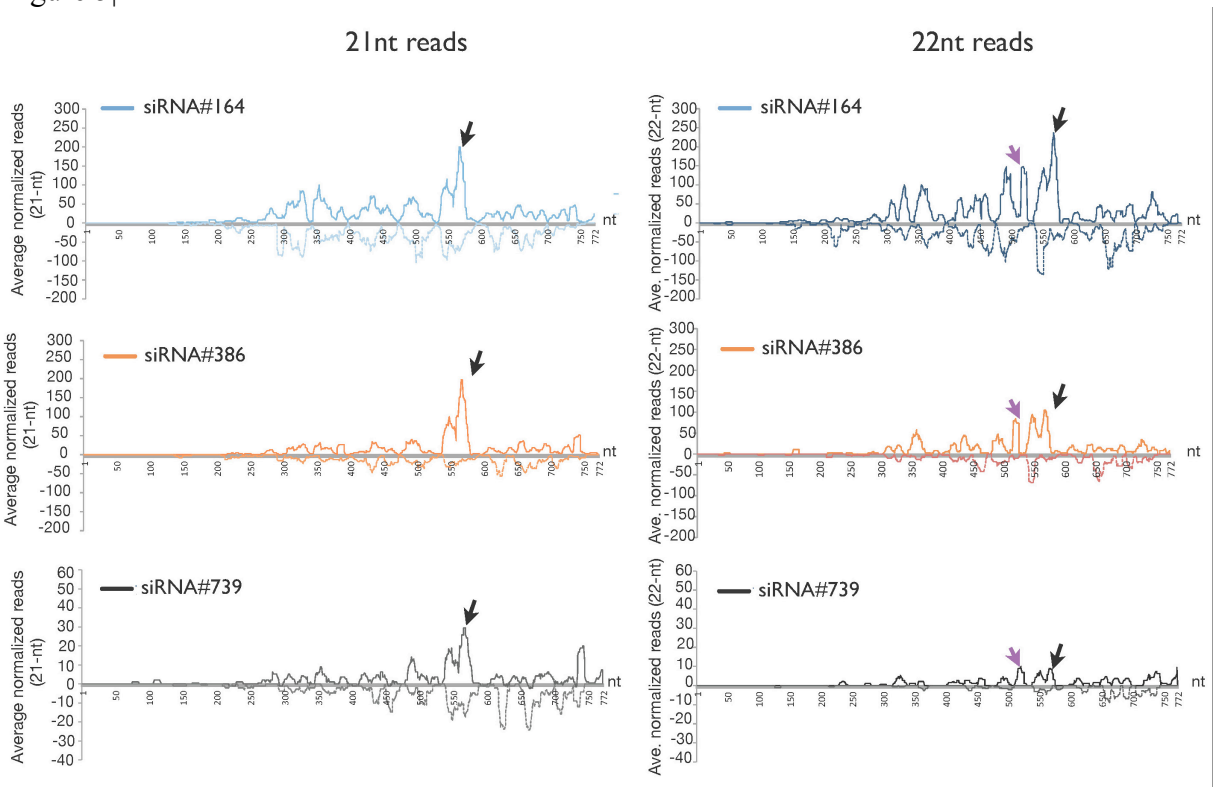

Figure 6|

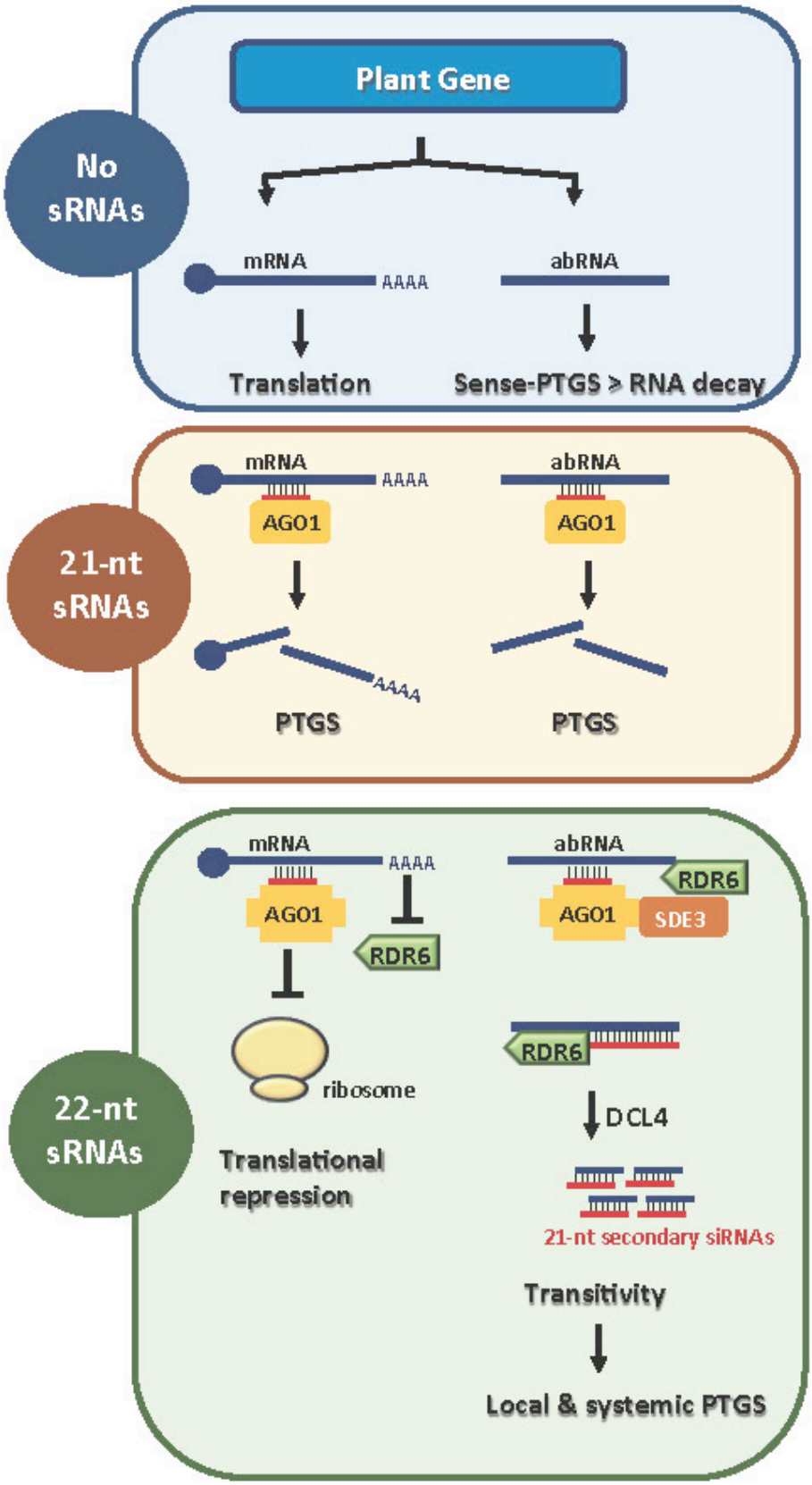
Plant Gene
No sRNAs
mRNA
AAAA
abRNA
Translation
Sense-PTGS > RNA decay
21-nt sRNAs
mRNA
AAAA
AGO1
abRNA
AGO1
AAAA
PTGS
PTGS
22-nt sRNAs
mRNA
AAAA
AGO1
RDR6
ribosome
Translational repression
abRNA
RDR6
AGO1
SDE3
RDR6
DCL4
21-nt secondary siRNAs
Transitivity
Local & systemic PTGS